ELSEVIER

International Journal of Mass Spectrometry 201 (2000) 307–320

International Journal of Mass Spectrometry

Structures and fragmentations of zinc(II) complexes of amino acids in the gas phase. I. Electrosprayed ions which are structurally different from their liquid phase precursors

Françoise Rogalewicz, Yannik Hoppilliard, Gilles Ohanessian*

Laboratoire des Mécanismes Réactionnels, UMR 7651 du CNRS, Ecole Polytechnique, 91128 Palaiseau Cedex, France

Received 21 December 1999; accepted 15 February 2000

Abstract

Zinc complexes of deprotonated amino acids (AA), denoted $[AA - H + Zn]^+$, are readily formed in the gas phase by electrospray. Their fragmentations can be studied by low energy collisional activation, yielding structural information about the gaseous ions. In this article we show that such ions may not have a structure similar to that of their liquid phase precursors. The simple case of the deprotonated methanol complex $[ZnOCH_3]^+$ is first studied in detail. The precursor of this ion in the desolvation process is $[(CH_3OH)ZnOCH_3]^+$. Accurate ab initio calculations show that the direct desolvation of this ion via methanol evaporation is a costly reaction, while rearrangement via β − H transfer to $[(CH_3OH)ZnH(OCH_2)]^+$ is much more favorable. Competitive evaporation of either methanol or methanal from the rearranged ion is also more favorable. Thus the $[Zn, O, C, H_3]^+$ ion observed corresponds to a two-ligand, hydride complex $[ZnH(OCH_2)]^+$. These computational results are fully consistent with experiments, either direct source or collision induced dissociation (CID) spectra. Analogous observations hold for the zinc complex of deprotonated glycine $[Gly - H + Zn]^+$. Detailed computations of the various possible structures of [Gly-H+Zn]+ and its precursor are consistent with the formation of rearranged structures, which are more stable than those of the initially formed species in solution. These structures are also adequate for explaining the low energy CID spectrum of $[(Gly - H)Zn]^+$. It is concluded that for electrosprayed ions in general, whenever the last desolvation steps are energetically costly, rearrangements may occur before evaporation of the last solvent molecule. The common wisdom that electrospray ionization is a gentle process which produces faithful images of solution phase structures is shown not to apply to certain categories of metal ions. (Int J Mass Spectrom 201 (2000) 307–320) © 2000 Elsevier Science B.V.

Keywords: Zinc ions; glycine; electrospray; isomerization; Ab initio

1. Introduction

Despite numerous studies on the fragmentation reactions of gaseous transition metal-cationized peptides, there have been comparatively few studies of the interaction of transition metal ions with α-amino acids (AA). Most of these studies have involved the formation of singly charged metal complexes by bombarding a mixture of an α-amino acid and a metallic salt with energetic particles. Harrison and co-workers have reported studies of the metastable ion fragmentation reactions of a variety of α-amino acids cationized by Cu^+ [1] or by Ni^+ upon fast atom bombardment (FAB) [2]. A report of the ion–molecule reactions of Cu^+ and Fe^+ with the 20 common

* Corresponding author. E-mail: gilles@dcmr.polytechnique.fr

PII S1387-3806(00)00226-8

α-amino acids, as studied by laser desorption/chemical ionization Fourier transform mass spectrometry has also appeared [3]. We have reported studies on the formation and decomposition in a plasma ion source (PD) of (1) the six aliphatic α-amino acids cationized with $FeCl^+$, Co^+, Ni^+, Cu^+ [4]; (2) several α-amino acids cationized with Cu^+ [5]. Several authors have observed that under FAB [1,2,6] or PD [4,5,7] ionization, the bombardment of an amino acid in mixture with a metallic salt in which the transition metal (Cat) is in its +2 oxidation state [(Cat(II)(] leads to formation of the $[AA + Cat]^+$ adduct ion in which the transition metal is in its +1 oxidation state. Such adducts involving a reduced metal ion have been previously observed when metal salts are added to organic compounds in desorption–ionization sources [8,9].

Ternary complexes of amino acids, Cat(II) or Cat(III) and basic ligands were obtained in the gas phase by electrospray or FAB ionization. Gatlin et al. have found that electrospraying methanol–water solutions of amino acids, a Cat(II) metal salt, Cu(II) [10–13], Co(II), Ni(II), Zn(II) [14], and a diimine ligand such as 2,2′-bipyridine (bpy) or phenanthroline results in facile formation of gas-phase ternary complexes of $[Cat(II)(AA - H)(bpy)]^+$. O'Hair [15] has reported on the gas-phase reactions of cationic complexes of glycine and cysteine with platinum(II) and terpyridine. Complexation of aluminium ions [Al(III) in glycerol] with α-amino acids has been studied by FAB mass spectrometry [16]. Finally, histidine complexes of doubly charged metal ions Cat^{2+} (Fe^{2+}, Co^{2+}, Ni^{2+}, and Zn^{2+}) have recently been studied by electrospray ionization [17].

Although numerous hypotheses have been formulated in the literature, the relationship between the fragmentation reactions, the metal binding sites and the metal binding affinities remain to be established.

In this series of articles, we show the determining role of the metal attachment sites on the formation and fragmentation of $[AA - H + Zn]^+$ ions. The electrospray of methanol–water solutions of mixtures of amino acids and $ZnCl_2$ leads to the formation of these Zn(II)-cationized molecular species. Herein we show that during the electrospray formation of such complexes, including those of the methanol solvent itself, isomerizations may occur before the final desolvation step. Accurate ab initio calculations are used to establish the occurrence of such rearrangements. Understanding these processes provides a rationale for the formation of $[M + H + Zn]^+$ (M = CH_3OH, AA), which can be used as a diagnostic ion for the formation of nonclassical structures.

2. Experimental and theoretical procedures

2.1. Experimental

Electrosprayed zinc complexes of methanol and glycine were formed from a glycine/$ZnCl_2$ mixture (500 and 250 μM, respectively) in a 50:50 volume water/methanol solution. Such concentrations are typical for the formation of metal complexes of amino acids. In such conditions, the pH is in the 6–6.5 range. Labeling experiments were performed by H/D exchanging all exchangeable hydrogens of glycine in a D_2O/CH_3OD solution. Solutions were introduced in the ion source with a syringe at a 10 μL/mn speed with a diffusion pump (Harvard, Southnatic, MA). L-Gly was purchased from Aldrich Chem. Co. (Saint Quentin Fallavier, France) and anhydrous $ZnCl_2$ was obtained from Merck KGaA (Darmstadt, Germany). All solvents were of HPLC grade.

All experiments were carried out on a triple quadrupole Quattro II mass spectrometer (Micromass, Manchester, UK). Source parameters were adjusted so as to optimize ion signals such as $[(Gly - H)Zn]^+$. Typical voltage values were: capillary 2.5–3.5 kV, counter electrode 0.1–0.3 kV, rf lens 0.7 eV, skimmer 1.5 V. Source spectra were recorded for two different values of the sampling cone voltage, 20 and 40 V.

Low energy collision induced dissociation (CID) of ion clusters such as $[(CH_3OH)ZnOCH_3]^+$ and $[(Gly)CH_3OZn]^+$ were performed with argon as the collision gas. The collision energy in the laboratory frame was set to 6 eV and the collision gas pressure was adjusted so as to diminish the parent ion intensity by 50%–70%. This experiment was repeated with the same pressure and a collision energy of 12 eV. Before

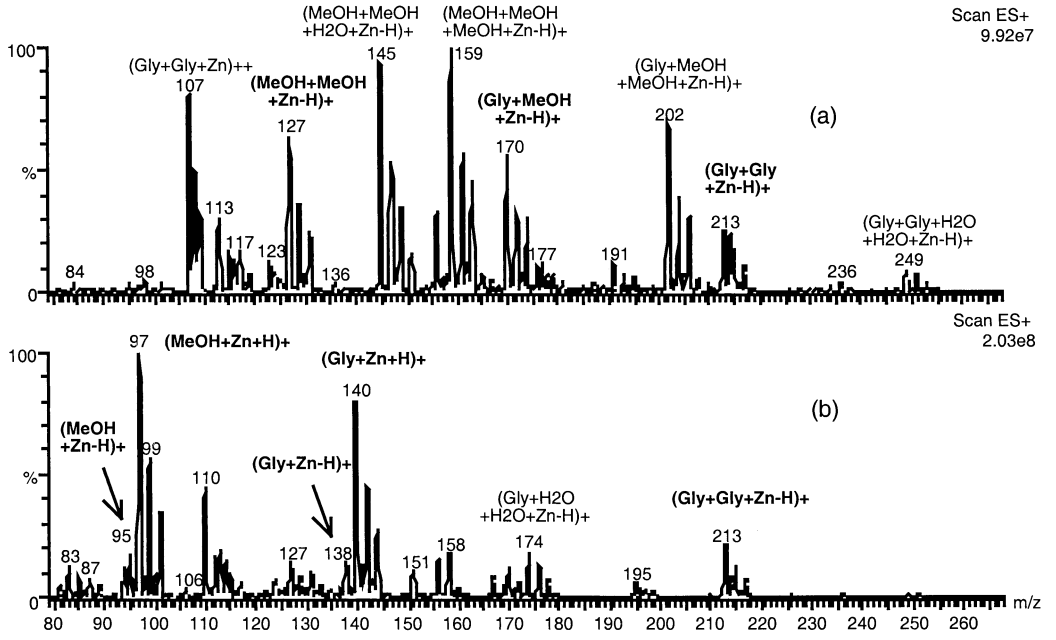

Fig. 1. Source spectra of a solution of glycine and $ZnCl_2$ in water/methanol solvent. Sampling cone voltage (a) $V_c = 20$ V and (b) $V_c = 40$ V.

each experiment, the resolution of the first quadrupole and the extraction cone voltage were set to maximize the intensity of the parent ion. This led to a cone voltage of 20 V and a collision gas pressure of $\sim 10^{-3}$ mbar.

2.2. Computational

Two basis sets were used in this study. For geometry optimizations and vibrational frequency calculations, the 6-31G* basis was used for H, C, N, and O, and the Wachters [14*s*9*p*5*d*1*f*/9*s*5*p*3*d*1*f*] was used for Zn [18]. This is referred to as basis1. For final energy calculations, basis2 consists in the 6-311+G(2*d*,2*p*) for H, C, N, and O, and the extended Wachters basis [15*s*11*p*6*d*2*f*/10*s*7*p*4*d*2*f*] for Zn. Geometry optimizations and vibrational frequency calculations were generally carried out at the frozen core second order Møller-Plesset MP2(FC)basis1 level, but for larger complexes, the Hartree-Fock (HF) level was used. Extensive tests described below showed that the use of HF geometries leads to very small errors in final energy calculations. Final energetics were obtained with MP2(FC)/basis2 wave functions at the MP2(FC)/basis1 or HF/basis1 geometries, a level denoted below as MP2(FC)/basis2//MP2(FC)/basis1 or MP2(FC)/basis2//HF/basis1, respectively. The GAUSSIAN94 program package [19] was used throughout.

3. Results

At low cone voltages such as $V_c = 20$ V, source spectra of the glycine/$ZnCl_2$ solution in the water/methanol solvent show (Fig. 1): (1) protonated species such as $[(Gly)_nH]^+ (n = 2–4)$, which we do not discuss herein, (2) cationized dimers and trimers of the types $[(Gly)_2Zn]^{2+}$, $[(Gly)_n(Gly - H)Zn]^+$, and $[(CH_3OH)_n - H + Zn]^+$ $(n = 1–3)$, (3) mixed oligomers such as $[(CH_3OH)_n(Gly)_m - H + Zn]^+$, $[H_2O)_n(Gly)_m - H + Zn]^+$ $(n = 1,2$ and $m = 1,2)$, and $[(CH_3OH)_2(H_2O) - H + Zn]^+$. Cationized monomers such as $[M - H + Zn]^+$ and [M +

$H + Zn]^+$ (M = Gly or CH_3OH) only appear with larger cone voltages (Fig. 1 with $V_c = 40$ V), when most solvent molecules have been removed. This has been previously observed in the electrospray spectra of mixtures of histidine with various metal salts [17]. With a cone voltage of 40 V, the relative intensity of $[M + H + Zn]^+$ appears to be at a maximum, and is much larger than that of $[M - H + Zn]^+$.

Zinc containing ions are characterized by multiple peaks due to the naturally occuring zinc isotopes of *m/z* 64, 66, 67, 68, and 70 with natural relative abundances of 48.89%, 27.81%, 4.11%, 18.56%, and 0.62%, respectively. In what follows, we will always mention the mass of a zinc containing ion with reference to the smallest *m/z*, which corresponds to the most abundant zinc isotope (*m/z* = 64). All ions identified as zinc-containing species showed intensity ratios consistent with the relative natural isotope abundances.

While the formation of deprotonated zinc complexes of organic molecules such as $[M - H + Zn]^+$ is anticipated since zinc is known, as many other metal ions, to deprotonate such species in neutral solutions [20], the presence of $[M + H + Zn]^+$ is rather hard to explain. Protonated M attached to a reduced Zn(0) atom would have a low MH^+/Zn binding energy, and is therefore not expected to be formed in significant intensity. As will be described below, formation of $[M + H + Zn]^+$ is actually due to extensive rearrangements within the precursor complex prior to final solvent evaporation. We have therefore studied in details the mechanism of the formation of $[M + H + Zn]^+$ ions. Another incentive for this study stemmed from a detailed computational study of $[Gly - H + Zn]^+$, aimed at obtaining a complete picture of the fragmentation of deprotonated Gly when attached to a zinc cation. Glycine bears a carboxylic acid function, which seems to be the natural site for deprotonation by a metal ion. Another potential site is the amine, since it is well known that metal complexation may significantly increase the Bronsted acidity of various functional groups. It turned out, however, that none of these structures could explain even the qualitative patterns of fragmentation observed under low energy collision conditions. Thus we were led to question the exact nature of the $[Gly - H + Zn]^+$ ions formed by electrospray. This article is devoted to such a study. As similar observations pertain to the methanol complexes of zinc $[(CH_3OH) + H + Zn]^+$ and $[(CH_3OH) - H + Zn]^+$, we start our computational investigation with these smaller cases which allow accurate calculations to be carried out. This is most helpful for devising appropriate computational levels for larger cases. Then we will proceed to the Gly complexes.

A full description of the $[Gly - H + Zn]^+$ potential energy surface, and an overall picture of the structures and fragmentations of the zinc complexes of deprotonated amino acids will be reported in the next articles of this series.

3.1. Formation and structure of $[(CH_3OH) + H + Zn]^+$ and $[(CH_3OH) - H + Zn]^+$

The source spectra shown in Fig. 1 display the formation of gaseous $[(CH_3OH)_2 - H + Zn]^+$ with a cone voltage $V_c = 20$ V, while at $V_c = 40$ V, an intense signal of $[(CH_3OH) + H + Zn]^+$ and a minor signal of $[(CH_3OH) - H + Zn]^+$ are obtained. These ions can also be studied in the tandem quadrupoles. A search of parent ions ($V_c = 20$ V) of $[(CH_3OH) + H + Zn]^+$ and $[(CH_3OH) - H + Zn]^+$ mainly leads to $[(CH_3OH)_2 - H + Zn]^+$. The low energy CID of selected $[(CH_3OH)_2 - H + Zn]^+$ were also studied. Typical spectra are displayed in Fig. 2. At low collision energy [$E_{lab} = 6$ eV, Fig. 2(a)], the dominant fragment ion is $[(CH_3OH) + H + Zn]^+$, with a minor amount of $[(CH_3OH) - H + Zn]^+$. At higher collision energy [e.g. $E_{lab} = 12$ eV, Fig. 2(b)], the intensity ratio between both fragments is close to 1. This is consistent with similar thresholds for formation of both ions, with that of $[(CH_3OH) + H + Zn]^+$ being somewhat smaller. The latter involves a formal loss of methanal, while formation of $[(CH_3OH) - H + Zn]^+$ corresponds to the elimination of a methanol molecule. In order to provide a rationale for these observations, a potential energy profile was obtained, as shown in Fig. 3. The MP2/basis1 optimized structures are shown in Fig. 4.

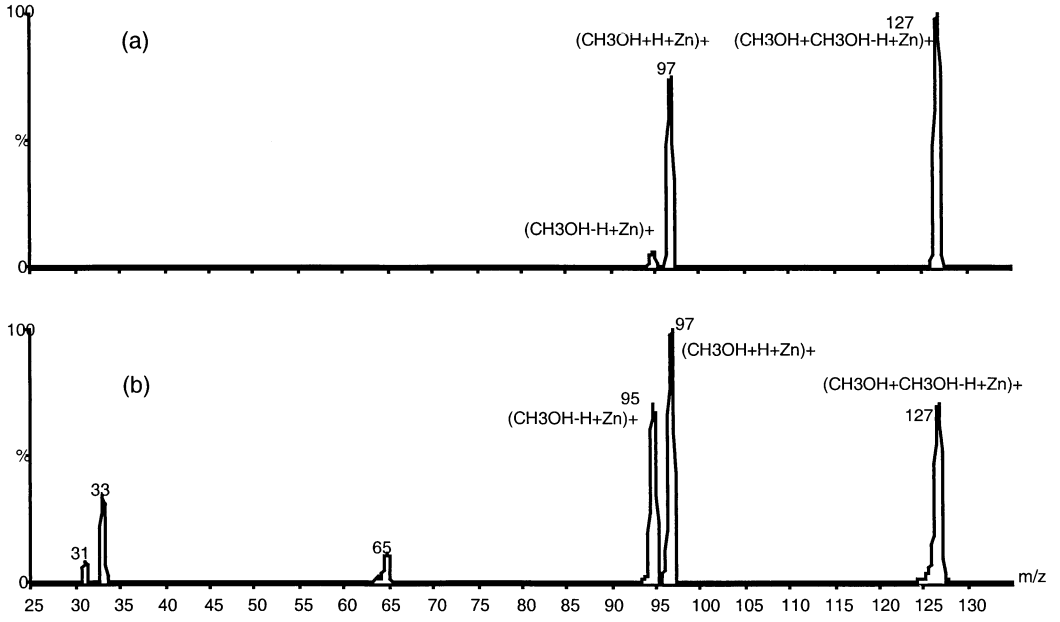

Fig. 2. CID spectra of $[(CH_3OH)_2 - H + Zn]^+$ (*m/z* 127). Laboratory frame collision energy (a) E_{lab} = 6 eV and (b) E_{lab} = 12 eV.

Final energy calculations were carried out at the MP2/basis2//MP2/basis1 level. The MP2/basis2//HF/basis1 level was also used systematically as a calibration step for calculations on larger complexes.

The initially formed complex in solution most probably involves one deprotonated methanol molecule together with intact CH_3OH solvent molecules. Solvent evaporation likely leads to a species of the form $[CH_3OZn(CH_3OH)]^+$. This is the stable species depicted on the left-hand side of Fig. 3. Solvent detachment from this ion is a costly process, worth 62.5 kcal/mol. There is a much more favorable process for this ion when collisionally activated: β-hydrogen transfer from the methanolate carbon to Zn. The activation barrier of 35.3 kcal/mol is so much lower in energy that direct methanol loss cannot occur at low collision energies. Hydrogen transfer leads to an isomeric ion in which there are three ligands on zinc, a hydride, H_2CO, and CH_3OH. The energy of this isomer is essentially identical to that of the "classical" form. From this structure, losses of methanal and methanol require 26.4 and 32.9 kcal/mol, respectively. This order is in keeping with that in

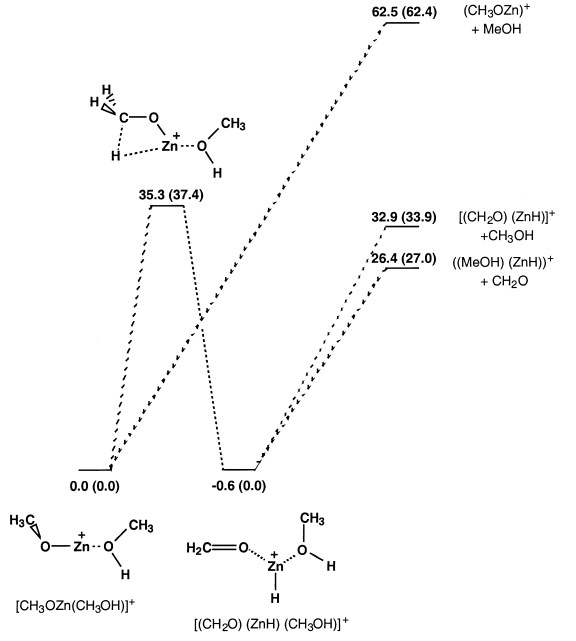

Fig. 3. Potential energy profile for the decomposition of $[CH_3OZn(CH_3OH)]^+$. Energies are at the MP2/basis2//MP2/basis1 level with MP2/basis2//HF/basis1 values in parentheses. All values in kilocalories per mole.

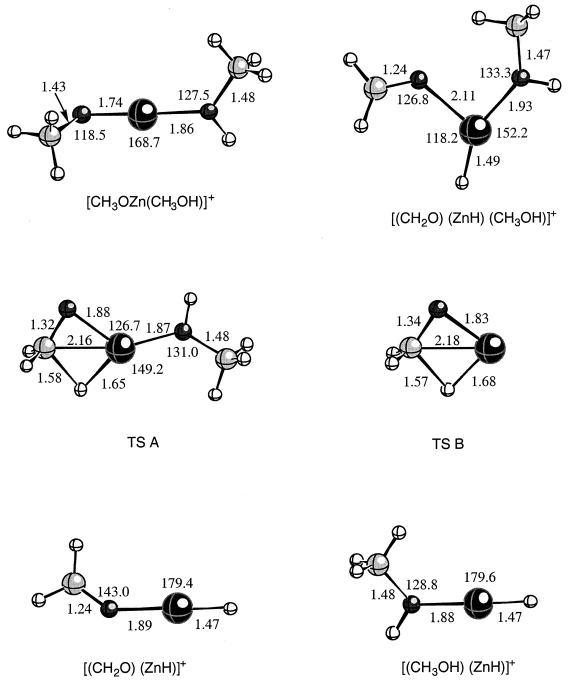

Fig. 4. Optimized structures of minima and transition state for the decomposition of $[CH_3OZn(CH_3OH)]^+$ at the MP2/basis1 level. Distances are in angstroms and angles in degrees.

one-ligand complexes of Zn^{2+}.[21] These results nicely explain the experimental observations: the lowest energy process involve β − H migration to the metal followed by detachment of methanal. The cost of methanal detachment is 32.9 or 6.5 kcal/mol smaller than that of methanol, in full agreement with the observation that the former is dominant at low collision energies and that both tend to have similar intensities at higher energies.

An important feature of these results is that direct desolvation is a costly process, while it is significantly easier from the rearranged isomer. The stronger interaction of CH_3OH with $[CH_3OZn]^+$ as compared to $[CH_2OZnH]^+$ may be explained by two different effects. First, the net metal charge (calculated from a natural population analysis of the MP2 wave function) in $[CH_3OZn]^+$ is 1.48, while in $[CH_2OZnH]^+$ it is reduced to 1.30 in the absence of a deprotonated oxygen ligand. This strongly diminishes the electrostatic, polarization, and charge transfer components of the interaction between zinc and methanol. Another difference comes from the coordination numbers in both isomers. In $[CH_3OZn]^+$ with only one ligand, methanol can bind to zinc with an OZnO angle of 180°, leading to very small ligand–ligand repulsions. In $[CH_2OZnH]^+$ the hydride and methanal ligands must depart from a linear arrangement upon attachment of methanol, in order to form a planar trigonal structure (see Fig. 4). This second effect also leads to a reduced binding energy for methanol. This reduction can be calculated as the energy difference between $[CH_2OZnH]^+$ at its optimum geometry and at its geometry in the methanol complex. At the MP2/basis2//MP2/basis1 level, this difference amounts to 17.0 kcal/mol.

The conclusion of this study is that neither $[CH_3OH + H + Zn]^+$ nor $[CH_3OH - H + Zn]^+$ have classical structures, but rather involve a hydride ligand. They are more appropriately written $[CH_3OHZnH]^+$ and $[CH_2OZnH]^+$, respectively. It is interesting to note that while the formation of $[CH_3OH - H + Zn]^+$ does not reveal the existence of a rearrangement since direct methanol loss from $[(CH_3OH)_2\ H + Zn]^+$ would lead to an isobaric ion, the presence of $[CH_3OH + H + Zn]^+$ in both the source spectra and CID of $[(CH_3OH)_2 - H + Zn]^+$ is diagnostic of this rather unusual process. Since the analogous ion is also formed with deprotonated glycine, we have investigated similar rearrangements in this case too.

Computational results obtained at the MP2/basis2//HF/basis1 level (indicated in parentheses in Fig. 3) show that HF geometries provide satisfactory accuracy. Calculations on the various possible isomers of $[Gly - H + Zn]^+$ and transition states of isomerization described below confirm the accuracy of this level. Therefore this level was used for solvated complexes. Finally, calculations were carried out on the rearrangement of CH_3OZn^+, i.e. an ion without the spectator methanol ligand. The transition state for the β − H migration is shown in Fig. 4. It is very similar to the corresponding structure with a methanol molecule added onto the metal. This step was found to involve a barrier of 34.1 and 36.2 kcal/mol at the MP2/basis2//MP2/basis1 and MP2/basis2/HF/basis1

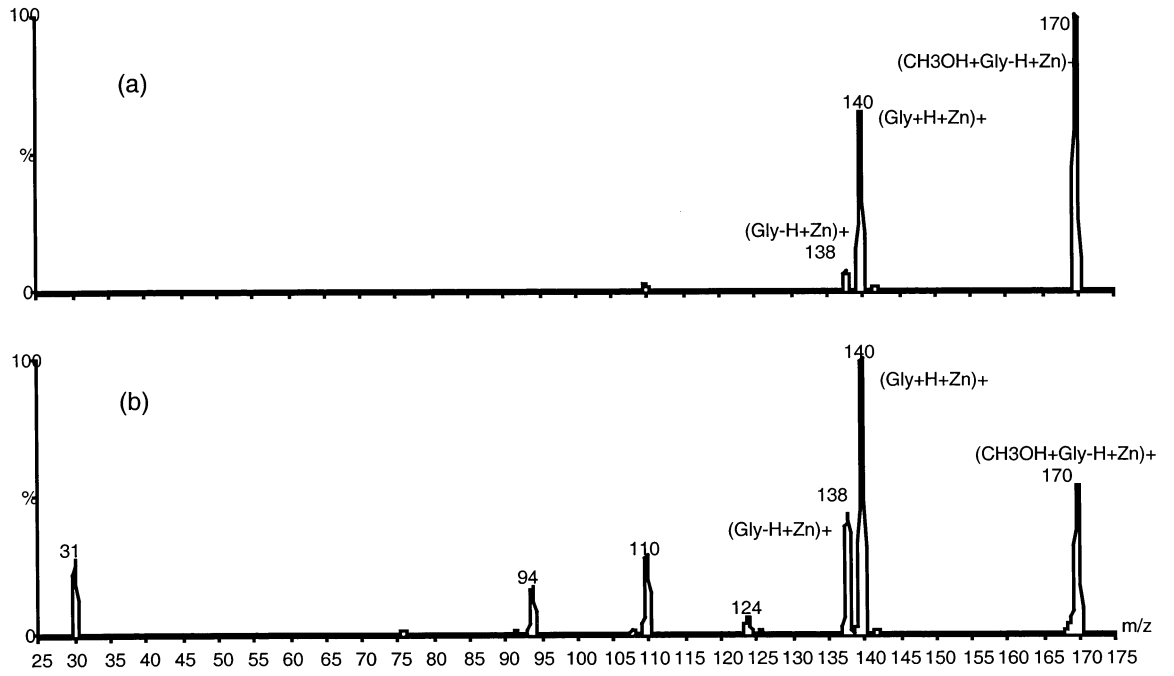

Fig. 5. CID spectra of $[CH_3OH + Gly - H + Zn]^+$ (*m/z* 170). Laboratory frame collision energy (a) E_{lab} = 6 eV and (b) E_{lab} = 12 eV.

levels, respectively. At each level, this is just 1.2 kcal/mol less than the barrier obtained when the spectator methanol molecule is included. Therefore analogous rearrangements in larger ions can be safely studied without the methanol molecule. For instance in the study of rearrangements of $[CH_3OH + Gly - H + Zn]^+$, we determined the geometries of transition states and stable species at the MP2/basis1 level without the methanol ligand, and then computed final energetics at the MP2/basis2//MP2/basis1 level. Calculations including a methanol molecule were carried out at the MP2/basis2//HF/basis1 level for the three starting structures [**1**, CH_3OH], [**4**, CH_3OH] and $[GlyZn)CH_3]^+$, two rearranged structures [**8**, CH_3OH] and [**9**, CH_3OH], and one transition state [**TS1-8**, CH_3OH] (see sec. 3.2).

3.2. Electrospray precursors of [Gly + H + Zn]$^+$ and [Gly − H + Zn]$^+$

At a cone voltage of 20 V, the zinc containing ions appear to be incompletely desolvated and are likely to correspond to preformed species in solution. In such low energy conditions, the precursor ions of $[Gly - H + Zn]^+$ (*m/z* 138) were found to be mainly *m/z* 170, plus 202 and 213, corresponding to $[CH_3OH + Gly - H + Zn]^+$, $[(CH_3OH)_2 + Gly - H + Zn]^+$ and $[(Gly)_2 - H + Zn]^+$, respectively. The fragmentations of $[CH_3OH + Gly - H + Zn]^+$ and $[(Gly)_2 - H + Zn]^+$ were studied at two values of the collision energy E_{lab} as shown in Fig. 5 for $[CH_3OH + Gly - H + Zn]^+$. The same experiments were repeated after H/D exchange of all exchangeable hydrogens.

With E_{lab} = 6 eV, an intense peak at *m/z* 140 corresponds to fragmentation of $[CH_3OH + Gly - H + Zn]^+$ into $[Gly + H + Zn]^+$ while $[Gly - H + Zn]^+$ is a very minor fragment. The latter becomes more intense with larger collision energies. This shows, as previously discussed in the methanol complex, that elimination of H_2CO is easier than that of CH_3OH. It is most likely that a methanal molecule arises from the methanolate rather than from the

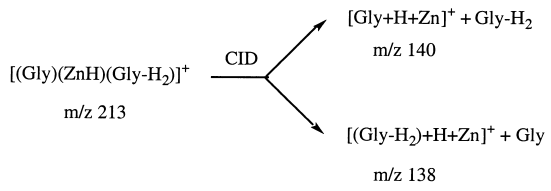

Scheme 1.

glycine fragment. Therefore here again a rearrangement must have occurred prior to fragmentation. With H/D exchanged ions, the fragment ion $[Gly + H + Zn]^+$ is shifted from *m/z* 140 to 143 while the parent ion is shifted from *m/z* 170 to 173.

Entirely similar results are obtained from CID experiments on $[(Gly)_2 - H + Zn]^+$ (*m/z* 213): formation of $[Gly + H + Zn]^+$ (*m/z* 140) occurs at lower collision energies than that of $[Gly - H + Zn]^+$ (*m/z* 138), and H/D exchange moves $[Gly + H + Zn]^+$ from *m/z* 140 to 143.

In analogy with the methanol case, formation of $[Gly + H + Zn]^+$ from $[(Gly)_2 - H + Zn]^+$ requires a rearrangement into $[(Gly)(ZnH)(Gly - H_2)]^+$. The deuteration experiments show that the hydrogen atom involved in the rearrangement is one of the $–CH_2–$ group. Competitive eliminations of Gly or $(Gly - H_2)$ from the rearranged structure lead to the observed product ions as shown in Scheme 1.

The concentration of Gly in the starting solution (500 μM) is low compared to that of CH_3OH which is used as the solvent. This leads to a much higher intensity of $[CH_3OH + Gly - H + Zn]^+$ compared to $[(Gly)_2 - H + Zn]^+$ in the source spectra. We have therefore studied the formation of $[Gly - H + Zn]^+$ and $[Gly + H + Zn]^+$ from $[CH_3OH + Gly - H + Zn]^+$ rather than from $[(Gly)_2 - H + Zn]^+$.

Several low energy structures can be envisioned for $[CH_3OH + Gly - H + Zn]^+$. It appears natural to consider first the deprotonation of the carboxylic acid function of Gly. However Zn^{2+} attachment dramatically increases the acidity of a functional group since the interaction of Zn^{2+} with a deprotonated ligand $(L - H)^-$ in $Zn(L - H)^+$ is much stronger than that with neutral L in ZnL^{2+}, i.e. reaction (1a) is much less endothermic than reaction (1b) [21]

$$ZnL^{2+} \rightarrow Zn(L - H)^+ + H^+ \quad (1a)$$

$$L \rightarrow (L - H)^- + H^+ \quad (1b)$$

This acidity reduction varies strongly from one ligand L to another. Therefore deprotonation at other functional sites must be taken into consideration. Deprotonation of the glycine amino group was therefore studied, as well as deprotonation of methanol. Geometry optimization of such species resulted in the structures depicted in 6a. Relative energies are indicated in Table 1. It can be seen that the relative energies are so close that all three structures are plausibly formed in solution, and may be considered as possible precursors of $[Gly + H + Zn]^+$ and $[Gly - H + Zn]^+$. A common feature to these three isomers is that direct desolvation is a rather unfavorable process. Indeed, methanol detachment from [**1**, CH_3OH] and [**4**, CH_3OH] is worth 54 kcal/mol, while glycine detachment from $[GlyZnOCH_3]^+$ is even more unfavorable, 90 kcal/mol. Therefore it is likely that there exists rearrangements with smaller energy demands, which may effectively compete with direct detachment.

Based on the methanol results, it is easy to understand the behavior of the methanol–deprotonated isomer. Since evaporation of Gly is a high energy process (see Table 1), a much better alternative is β − H migration from the methanolate carbon to zinc as shown in Scheme 2. The activation barrier for this

Table 1
Relative energies of $[CH_3OH + Gly + Zn - H]^+$ isomers, the transition state connecting [**1**, CH_3OH] to [**8**, CH_3OH], and the corresponding dissociated complexes in kcal/mol

Isomer	HF/basis1	MP2/basis2 //HF/basis1
[**1**, CH_3OH]	0.0	0.0
1 + CH_3OH	55.9	53.9
[**4**, CH_3OH]	4.7	2.2
4 + CH_3OH	58.4	53.9
$[GlyZnOCH_3]^+$	−2.4	−2.3
Gly + $ZnOCH_3^+$	92.0	89.9
[**8**, CH_3OH]	21.9	22.6
8 + CH_3OH	44.1	46.7
[**9**, CH_3OH]	14.9	15.2
9 + CH_3OH	38.3	39.8
[**TS 1–8**, CH_3OH]	52.5	45.4

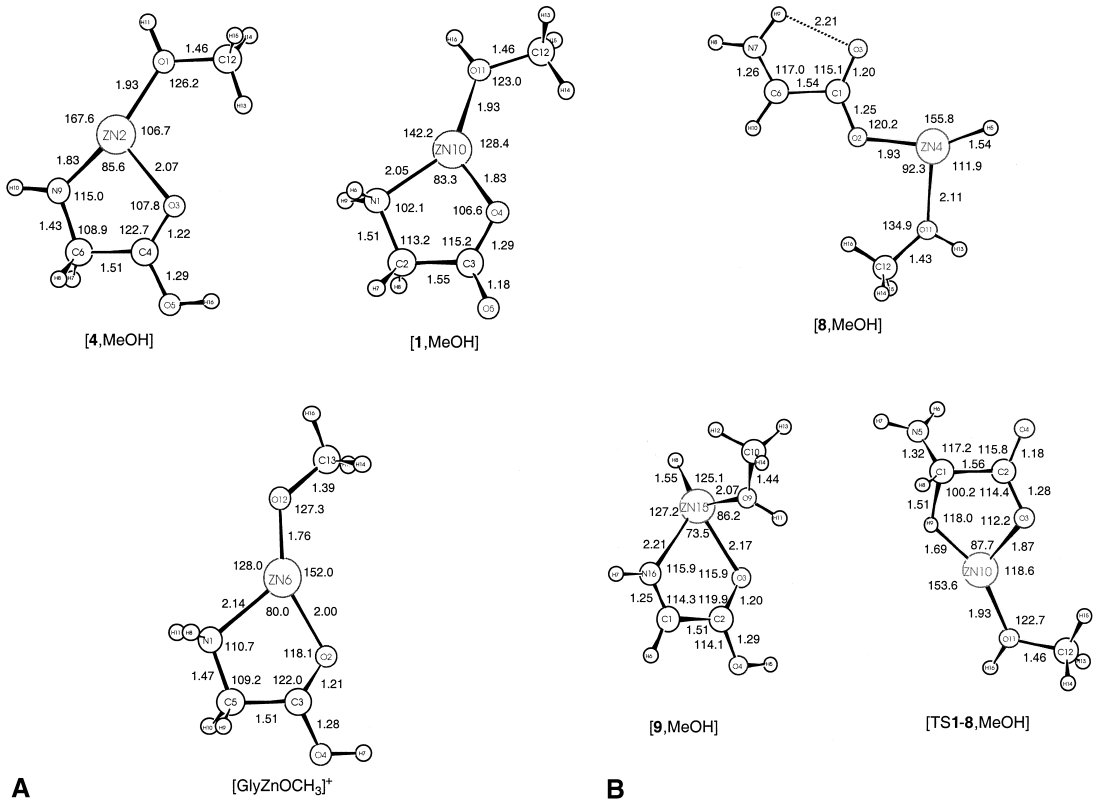

Fig. 6. Optimized structures of $[CH_3OH + Gly - H + Zn]^+$ at the HF/basis1 level. Distances are in angstroms and angles in degrees.

process may be equated to that in either $[ZnOCH_3]^+$ or $[(CH_3OH)ZnOCH_3]^+$, ca 35 kcal/mol.

From the rearranged structure, elimination of methanal is the only favorable channel, in agreement with the lack of $[H_2CO + H + Zn]^+$ (which would result from elimination of Gly) in the CID spectrum. This pathway is also in agreement with the results of the deuteration experiments since the three exchangeable hydrogens remain in the fragment ion.

Fragmentation of [**1**, CH_3OH] and [**4**, CH_3OH] is

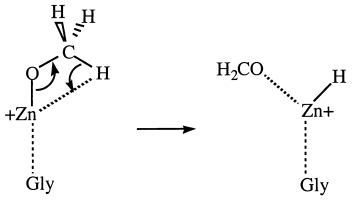

Scheme 2.

significantly more complex since there are many conceivable rearrangements within Gly. Therefore in the next sections, we first establish the structure of the low energy isomers of $[Gly - H + Zn]^+$, and then consider interconversions between some of them.

3.3. Structures of $[Gly - H + Zn]^+$

A large number of structures can be envisioned for $[Gly - H + Zn]^+$. We have considered structures which formally result from either attachment of Zn^{2+} to deprotonated glycine, or from attachment of ZnH^+ to dehydrogenated glycine. In each case, there are three possible sites of deprotonation or dehydrogenation: the carboxylic, amino, and α methylene groups. The metal has always been attached to the deprotonated function since this leads to very large stabilization energies. Metal chelation has been enforced as

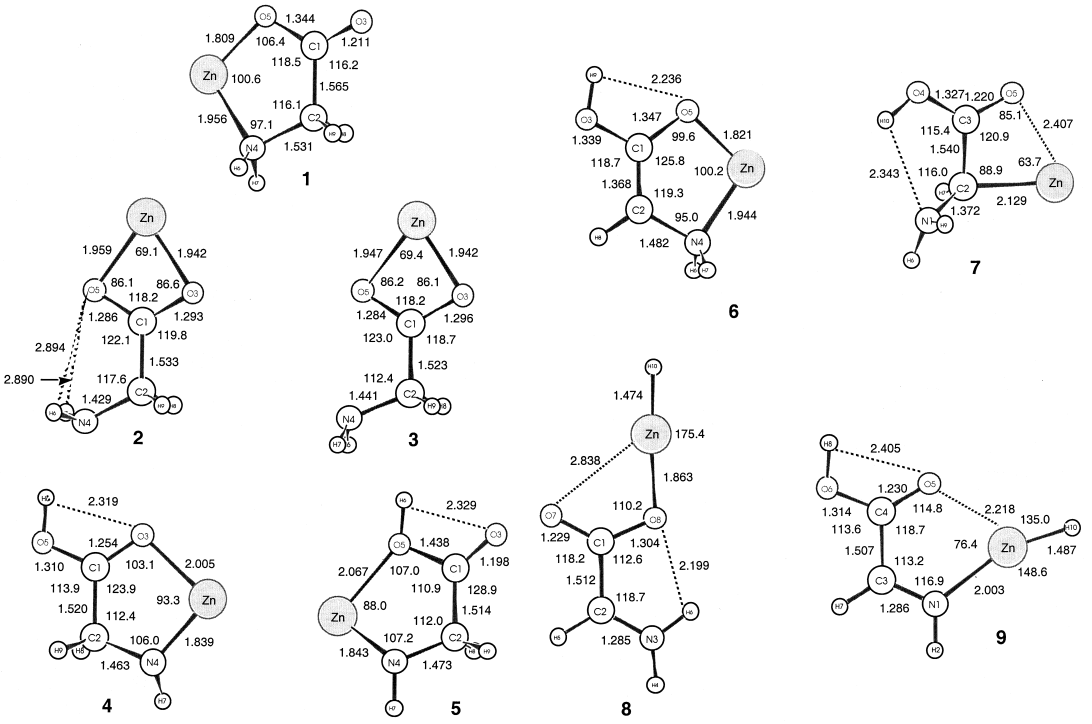

Fig. 7. Optimized structures of [Gly − H + Zn]$^+$ at the MP2/basis1 level. Distances are in angstroms and angles in degrees.

much as possible, while maintaining intramolecular hydrogen binding whenever possible. This leads to nine isomers, whose MP2/basis1 optimized geometries are displayed in Fig. 7. Their relative energies at various computational levels are gathered in Table 2.

Isomers **1**, **2**, and **3**, in which the metal ion is attached to a carboxylate group, would appear to be the most likely to be formed in solution. Isomer **1** involves metal chelation between the deprotonated oxygen and the nitrogen atoms. It involves a short Zn–O bond, due to the large electrostatic interaction. Isomers **2** and **3** involve the interaction of zinc with both oxygens of the carboxylate group. They differ by the pyramidalization of the amino group. As a consequence, there is an additional stabilization through intramolecular hydrogen binding in **2**, at the expense of a reduced overall dipole moment of the Gly − H fragment. The small energy difference indicates that the favorable charge–dipole interaction in **3** largely compensates for the lack of intramolecular hydrogen bonds as in **2**. Both are significantly less stable than **1**.

Another type of structure results from deprotonation of the amino group, as shown in **4** and **5**. Both involve a short Zn–N bond. In the absence of zinc, amine deprotonation has been computed to be less favorable than formation of a carboxylate by 54 kcal/mol at the MP2(FC)/6-31+G* level. The small energy difference between **1** and **4** shows that, not only does zinc increase dramatically the acidity of the functional group to which it is attached, but also that relative acidities are considerably changed. As for other metal ion complexes of glycine, chelation to the carbonyl oxygen as in **4** is significantly more favorable than to the hydroxyl oxygen as in **5**.

As shown by the relatively high energies of structures **6** and **7**, deprotonation at carbon is unfavorable.

Finally, attachment of ZnH^+ to dehydrogenated Gly was considered. This resulted in structures **8** and **9**. These turn out to be the most stable of all isomers in the gas phase.

The relative stabilities of all isomers were computed at several levels (see Table 2). While the

Table 2
Relative energies of $[Gly + Zn - H]^+$ isomers and interconversion transition states in kcal/mol

Isomer	HF/basis1	MP2/basis1 //HF/basis1	MP2/basis1	MP2/basis2// MP2/basis1	MP2/basis2 //HF/basis1
1	0.0	0.0	0.0	0.0	0.0
2	6.3	11.1	12.3	13.9	
3	7.4	12.2	13.4	14.3	
4	2.5	8.3	8.1	1.2	−0.1
5	22.1	22.3	21.6	17.7	
6	13.3	14.8	15.6	11.3	10.5
7	22.0	13.4	13.4	13.7	
8	−11.8	−11.1	−11.5	−7.1	−7.2
9	−17.6	−15.9	−15.8	−13.7	−14.1
9″	−7.5		−3.9	−0.9	
9″	−9.9		−7.5	−6.8	
TS 1–8	52.3		50.8	44.4	45.1
TS 9–9′	0.5		2.0	2.7	
TS 9–9″	23.2		20.9	23.4	24.3
TS 9″–8	9.4		2.0	4.7	

HF/basis1 level is comparatively inaccurate, the MP2/basis1//HF/basis1 and MP2/basis1 levels are in good agreement. This shows that HF/basis1 and MP2/basis1 geometries are very similar, and reinforces our previous conclusion that the HF/basis1 level can be safely used for geometry optimization. The need for an extended basis set is also clear from Table 2, since some of the MP2/basis2//MP2/basis1 relative energies differ significantly from the MP2/basis1 values. For instance the energy difference between isomers **1** and **4** and is reduced from 8.1 to 1.2 kcal/mol. The computational level of choice for larger cases is therefore MP2/basis2//HF/basis1.

It is unlikely that isomers **8** and **9** are formed in solution since they do not arise from simple deprotonation of Gly. The species which are most likely to be formed in solution appear to be isomers **1** and **4**. Given their structural similarity, their relative stabilities may be close to those computed in the gas phase. Isomers and **8** and **9** are related to **1** and **4**, respectively, by hydrogen transfer from the glycine CH_2 group to the metal. Thus they are candidates for rearranged structures formed before desolvation of $[Gly - H + Zn]^+$ precursors, in analogy with the methanol case.

3.4. Isomerization of $[Gly - H + Zn]^+$

Starting from the low energy structures described above, a variety of isomerization pathways may be considered. Still other isomers exist, with the glycine backbone broken down into two or three fragments attached to the metal. We have considered a number of pathways for such isomerizations, in an attempt to interpret the observed fragmentations of $[Gly - H + Zn]^+$ under low energy CID conditions. A full description of this exploration of the potential energy surface will be reported in a separate paper. Herein we focus on some of the isomerizations which may occur within the incompletely desolvated $[CH_3OH + Gly - H + Zn]^+$ precursor. For this purpose, we restrict ourselves to a rearrangement which starts with an analogue of the $\beta - H$ migration previously described in the methanol case, and then proceeds further until desolvation can occur easily. This pathway, from isomer **1** to **8** to **9**, is depicted on Fig. 8 and the optimized structures are displayed on Fig. 9. The energies of the transition states and intermediates are gathered in Table 2.

Starting from **1**, H migration from the methylene group to Zn leads to isomer **8**. This is very similar to the $\beta - H$ transfer from methanolate in

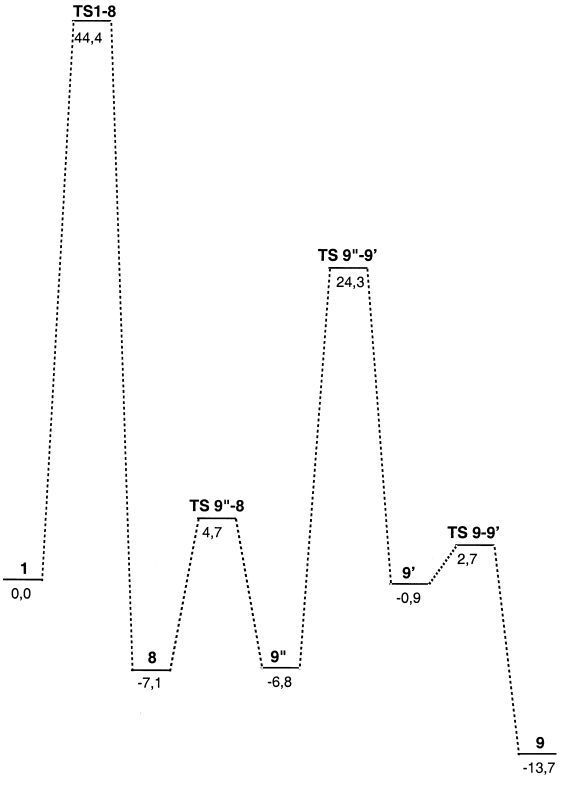

Fig. 8. Potential energy profile for the isomerization of [Gly − H + Zn]$^+$. Energies are at the MP2/basis2//MP2/basis1 level. All values in kilocalories per mole.

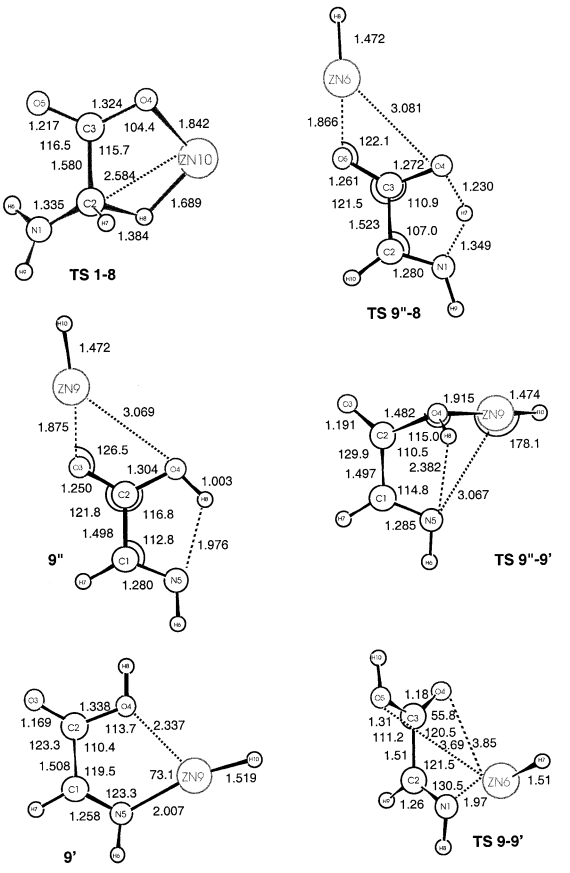

Fig. 9. Optimized structures of additional minima and transition states for the isomerization of [Gly − H + Zn]$^+$ at the MP2/basis1 level. Distances are in angstroms and angles in degrees.

$[(CH_3OH)_2 - H + Zn]^+$ (see Figs. 3 and 4) except that metal chelation between oxygen and nitrogen in **1** is more constraining and prevents an in-plane H migration. As a consequence the activation barrier lies higher in energy, 44.4 kcal/mol higher than **1**. When H transfer to the metal is complete, the backbone of dehydrogenated Gly has a delocalized π system, leading to a strong preference for planarity. This prevents metal chelation to nitrogen, therefore there is a migration of the metal toward the carboxylate end. Isomerization of **8** into **9** requires several elementary steps, including H migration from N to O, rotation around the C–OH bond bringing ZnH^+ from the acid group back to a chelating position between O and N, and finally rotation around the CC bond. While a concerted mechanism cannot be a priori excluded, we have only been able to find the stepwise pathway described in Figs. 8 and 9. The highest barrier of the three being 24.3 kcal/mol relative to **1**, the rate limiting step in the overall mechanism is that connecting **1** and **8**.

3.5. Desolvation versus rearrangement in $[CH_3OH + Gly - H + Zn]^+$

We are now able to put together the various processes described previously to examine the fate of the isomers of $[CH_3OH + Gly - H + Zn]^+$ when collisionally activated. Recall that we have considered three isomers, which are so close in energy that all three must be taken into account as possible precursors of [Gly − H + Zn]$^+$. We have restricted our

investigations to [**1**, CH_3OH] in this work. Direct detachment of methanol requires 54 kcal/mol, which appears large enough to allow rearrangements to take place. The pathway leading from **1** to **8** and **9′** via **9′** and **9″** involves four activation barriers, the highest of which lies 44.4 kcal/mol above [**1**, CH_3OH]. While this 10 kcal/mol differences is not as spectacular as that for the methanol-deprotonated isomer, it is large enough that low energy collisions will undoubtedly permit isomerization to take place. In order to check that methanol solvation does not Perturb this scenario significantly, we have calculated the methanol-solvated structures and energetics of [**8**, CH_3OH], [**9**, CH_3OH], and [**TS1-8**, CH_3OH]. The results are given in Table 1 and Fig. 6B. For [**8**, CH_3OH], in which the formal positive charge is on nitrogen, we have also considered an isomer in which methanol solvates a N–H bond; it is 3 kcal/mol less stable than the isomer reported. The barrier connecting **1** and **8** is found to be essentially unchanged when methanol is attached to Zn (see Tables 1 and 2). From isomers [**8**, CH_3OH] and [**9**, CH_3OH], methanol detachment can occur with energy demands of 24.1 and 24.6 kcal/mol, respectively, i.e. much lower than from [**1**, CH_3OH]. Thus [**1**, CH_3OH] is another case where isomerization precedes, and facilitates, the final desolvation step. Other pathways, starting both from [**1**, CH_3OH] and [**4**, CH_3OH], provide even more favorable rearrangement channels. These eventually lead to the breaking of the glycine backbone, which prepares for fragmentations in good agreement with the CID spectra of $[Gly - H + Zn]^+$. The details of these investigations will be reported in the next paper of this series.

4. Conclusions

This work shows that the formation of gaseous zinc complexes by electrospray may lead to unusual structures, resulting from isomerizations prior to evaporation of the last solvent molecule. This runs contrary to the common wisdom that gaseous electrosprayed ions are a direct image of solvated ions in solution. In fact, solvent evaporation requires significant amounts of energy, much like collisional activation in the "low energy" range (typically several electron volts). The last steps of solvent evaporation are expected to be the most demanding energetically, since such molecules are within the first solvation shell of the ion. In most cases of metal ions for which binding energetics are known, the last molecule is the most strongly bound. Therefore it is likely that it is in the very final stages of desolvation that isomerization will occur if any.

Much work, both experimental and theoretical, is needed to fully grasp the scope and generality of these conclusions. Yet a few criteria emerge which might help devising future work in this direction. Isomerization within an incompletely desolvated ion is likely to occur if the following conditions are fulfilled. (1) The desolvation of a solvent molecule, particularly the last one, must be energetically demanding. This is most likely to occur in metal-containing ions, and in general when the charge is highly localized. (2) There must exist rearrangements with low energy barriers. The β − H migrations described herein are only one classical example of easy processes in organometallic chemistry. They have been extensively studied in the reactions of singly charged transition metal cations with organic molecules [22]. The presence of open electronic shells [as opposed to the closed shell d^{10} structure of Zn(II)] may lead to lower activation barriers. In fact, Kohler and Leary [23] have observed the formation of analogous mixtures of $[(CH_3OH) + H + Cat]^+$ and $[(CH_3OH) - H + Cat]^+$ (Cat = Mn, Co). Whenever H migration to the metal is involved, formation of $[M + H + Zn]^+$ together with $[M - H + Zn]^+$ may serve as a diagnostic for the existence of a rearrangement. (3) Desolvation from the rearranged structure must be easier than for the parent structure. This is easily achieved if isomerization leads to a species in which the metal charge is reduced, or in which the metal coordination sphere is significantly more crowded. In the first case the intrinsic metal-ligand binding energy is reduced, while relief of steric strain is at work in the second.

Experiments and calculations described in this work establish the existence of isomerizations in the deprotonated, incompletely desolvated zinc complexes of methanol and glycine. In future papers of

this series, we will examine the occurrence and influence of such isomerizations on the fragmentations of zinc complexes of glycine and other amino acids.

Acknowledgement

This work was supported by a grant of computer time at the Institut de Développement et de Ressources en Informatique Scientifique (IDRIS, project no. 990543).

References

[1] D. Wen, T. Yalcin, A.G. Harrison, Rapid Commun. Mass Spectrom. 9 (1995) 1155.
[2] T. Yalcin, J. Wang, D. Wen, A.G. Harrison, J. Am. Soc. Mass Spectrom. 8 (1997) 748.
[3] Q.P. Lei, J. Amster, J. Am Soc. Mass Spectrom. 7 (1996) 722.
[4] S. Bouchonnet, Y. Hoppilliard, G. Ohanessian, J. Mass Spectrom. 30 (1995) 172.
[5] H. Lavanant, Y. Hoppilliard, J. Mass Spectrom. 32 (1997) 1037.
[6] P.M. Lausarot, G.A. Vaglio, Org. Mass Spectrom. 26 (1991) 51.
[7] H. Grade, R.G. Cooks, J. Am. Chem. Soc. 100 (1978) 5615.
[8] J.C. Blais, N. Hebert, G. Bolbach, Int. J. Mass Spectrom. Ion Processes 88 (1988) 29.
[9] H. Lavanant, Y. Hoppilliard, Rapid Commun. Mass Spectrom. 12 (1998) 1137.
[10] C.L. Gatlin, F. Turecek, T. Vaisar, J. Am. Chem. Soc. 117 (1995) 3637.
[11] C.L. Gatlin, F. Turecek, T. Vaisar, J. Mass Spectrom. 30 (1995) 775.
[12] C.L. Gatlin, F. Turecek, T. Vaisar, J. Mass Spectrom. 30 (1995) 1605.
[13] C.L. Gatlin, F. Turecek, T. Vaisar, J. Mass Spectrom. 30 (1995) 1617.
[14] C.L. Gatlin, F. Turecek, T. Vaisar, J. Mass Spectrom. 30 (1995) 1636.
[15] R.A.J. O'Hair, Eur. Mass Spectrom. 3 (1997) 390.
[16] M. Saraswathi, J.M. Miller, Rapid Commun. Mass Spectrom. 10 (1996) 1706.
[17] H. Lavanant, E. Hecquet, Y. Hoppilliard, Int. J. Mass Spectrom. Ion Processes 185/186/187 (1999) 11.
[18] A.J.H. Wachters, J. Chem. Phys. 52 (1970) 1033.
[19] GAUSSIAN94 (revision B.1), M.J. Frisch, G.W. Trucks, H.B. Schlegel, P.M.W. Gill, B.G. Johnson, M.A. Robb, J.R. Cheeseman, T.A. Keith, G.A. Petersson, J.A. Montgomery, K. Raghavachari, M.A. Al-Laham, V.G. Zakrzewski, J.V. Ortiz, J.B. Foresman, J. Cioslowski, B.B. Stefanov, A. Nanayakkara, M. Challacombe, C.Y. Peng, P.Y. Ayala, W. Chen, M.W. Wong, J.L. Andres, E.S. Replogle, R. Gomperts, R.L. Martin, D.J. Fox, J.S. Binkley, D.J. Defrees, J. Baker, J.J.P. Stewart, M. Head-Gordon, C. Gonzalez, J.A. Pople, Gaussian Inc., Pittsburgh, PA, 1995.
[20] Deprotonation in the gas phase is also possible. See M. Peschke, A.T. Blades, P. Kebarle, Int. J. Mass Spectrom. Ion Processes 185/186/187 (1999) 685.
[21] See, e.g. D.R. Garmer, N. Gresh, J. Am. Chem. Soc. 116 (1994) 3556, and references therein.
[22] K. Eller, H. Schwarz, Chem. Rev. 91 (1991) 1121, and references therein.
[23] M. Kohler, J.A. Leary, J. Am. Soc. Mass Spectrom. 8 (1997) 1124.